Engineering Water To Act as an Active Site Acid Catalyst in a Soluble Fumarate Reductase†

Christopher G. Mowat,‡,§ Katherine L. Pankhurst,‡ Caroline S. Miles,§ David Leys,|| Malcolm D. Walkinshaw,§ Graeme A. Reid,§ and Stephen K. Chapman*,‡

Department of Chemistry, University of Edinburgh, West Mains Road, Edinburgh EH9 3JJ, U.K., Institute of Cell and Molecular Biology, University of Edinburgh, Mayfield Road, Edinburgh EH9 3JR, U.K., and Department of Biochemistry, Adrian Building, University of Leicester, University Road, Leicester LE1 7RH, U.K.

Received April 29, 2002; Revised Manuscript Received July 26, 2002

ABSTRACT: The ability of an arginine residue to function as the active site acid catalyst in the fumarate reductase family of enzymes is now well-established. Recently, a dual role for the arginine during fumarate reduction has been proposed [Mowat, C. G., Moysey, R., Miles, C. S., Leys, D., Doherty, M. K., Taylor, P., Walkinshaw, M. D., Reid, G. A., and Chapman, S. K. (2001) *Biochemistry 40,* 12292−12298] in which it acts both as a Lewis acid in transition-state stabilization and as a Brønsted acid in proton delivery. This proposal has led to the prediction that, if appropriately positioned, a water molecule would be capable of functioning as the active site Brønsted acid. In this paper, we describe the construction and kinetic and crystallographic analysis of the Q363F single mutant and Q363F/R402A double mutant forms of flavocytochrome c_3, the soluble fumarate reductase from *Shewanella frigidimarina*. Although replacement of the active site acid, Arg402, with alanine has been shown to eliminate fumarate reductase activity, this phenomenon is partially reversed by the additional substitution of Gln363 with phenylalanine. This Gln → Phe substitution in the inactive R402A mutant enzyme was designed to "push" a water molecule close enough to the substrate C3 atom to allow it to act as a Brønsted acid. The 2.0 Å resolution crystal structure of the Q363F/R402A mutant enzyme does indeed reveal the introduction of a water molecule at the correct position in the active site to allow it to act as the catalytic proton donor. The 1.8 Å resolution crystal structure of the Q363F mutant enzyme shows a water molecule similarly positioned, which can account for its measured fumarate reductase activity. However, in this mutant enzyme Michaelis complex formation is impaired due to significant and unpredicted structural changes at the active site.

Bacterial fumarate reductases allow the use of fumarate as a terminal electron acceptor in anaerobic respiration. Within this enzyme family, there are essentially two types of fumarate reductase. The majority of organisms utilize a membrane-bound complex that is closely related to succinate dehydrogenase and uses iron−sulfur centers and FAD[1] as cofactors (*1*, *2*). However, in *Shewanella* species a soluble periplasmic, tetraheme, FAD-containing enzyme (flavocytochrome c_3) is produced (*3*). Despite these differences, the crystal structures of fumarate reductases from *Escherichia coli* [PDB entry 1FUM (*1*)], *Wolinella succinogenes* [1QLA, 1QLB (*4*), and 1E7P (*5*)], and *Shewanella* species [1QJD (*6*), 1D4E (*7*), and 1QO8 (*8*)] show a clear conservation of the active site architecture. This conservation of the active site around the FAD is consistent with a common mechanism for fumarate reduction. Indeed, there is now a considerable body of evidence for the operation of a universal mechanism for fumarate reduction throughout this family of enzymes (*6*, *9*, *10*).

The structure of the enzyme from *Shewanella frigidimarina* [1QJD (*6*)] is at 1.8 Å resolution, the highest-resolution structure available for any of the fumarate reductases. On the basis of this structure, a mechanism was proposed involving the use of an arginine residue (Arg402) as the active site acid catalyst (*6*). Arg402 transfers protons to the substrate as part of a proton delivery pathway involving Arg381 and Glu378 (*9*). More recently, the role of Arg402 has been investigated further by site-directed mutagenesis, and a dual role has been proposed which takes advantage of the unique ability of the residue to act as both a Lewis acid (stabilizing the build-up of negative charge in the transition state) and a Brønsted acid (delivering a proton to the substrate) (*10*). Using this mechanism, we have proposed the existence of two separate positions at the active site of

† This work was supported by the UK Biotechnology and Biological Sciences Research Council (BBSRC) and by the Wellcome Trust-funded Edinburgh Protein Interaction Centre (EPIC). K.L.P. acknowledges studentship funding from the EPSRC. Synchrotron access at EMBL Hamburg was supported by the European Community-Access to Research Infrastructure Action of the Improving Human Potential Programme to the EMBL Hamburg Outstation (Contract HPRI-CT-1999-00017).

* To whom correspondence should be addressed: Department of Chemistry, University of Edinburgh, West Mains Road, Edinburgh EH9 3JJ, U.K. E-mail: S.K.Chapman@ed.ac.uk. Fax and phone: (44) 131 650 4760.

‡ Department of Chemistry, University of Edinburgh.

§ Institute of Cell and Molecular Biology, University of Edinburgh.

|| University of Leicester.

[1] Abbreviations: Fcc_3, flavocytochrome c_3; Q363F/R402A, glutamine 363 → phenylalanine, arginine 402 → alanine double mutation; Q363F, glutamine 363 → phenylalanine single mutation; FAD, flavin adenine dinucleotide.

10.1021/bi0203177 CCC: $22.00
Published on Web 09/14/2002

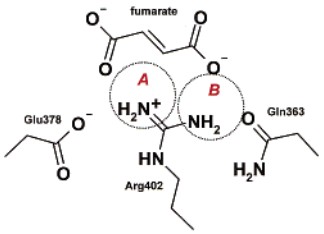

FIGURE 1: Schematic representation of positions A and B in the active site of flavocytochrome c_3. It can be seen that the bifurcated side chain of Arg402 results in the occupation of position A and position B by Brønsted acid and Lewis acid groups, respectively, thus explaining its efficiency as the acid catalyst in fumarate reductase.

fumarate reductase (Figure 1): position A, which when occupied by a species capable of Brønsted acid function may act as the proton donor during succinate formation, and position B, which if occupied by a Lewis acid species can stabilize the transition state and consequently increase the rate of catalysis (*10*). This conclusion was reached as a result of kinetic and structural studies on three Arg402-substituted forms of flavocytochrome c_3. Replacement of Arg402 with lysine or tyrosine was shown to introduce a Brønsted acid function at position A of the active site leading to active enzymes, albeit with greatly decreased activity. However, replacement of Arg402 with alanine produced an enzyme with no measurable catalytic activity. The structure of the R402A mutant enzyme reveals the existence of a water molecule at position B but no ordered entity at position A. This explained the lack of fumarate reductase activity in the R402A mutant (*10*). Our "two-position" model led us to propose that if the R402A enzyme could be re-engineered to place a water molecule in position A (with conservation of the arrangement of the remainder of the proton delivery pathway), then fumarate reductase activity would be restored. To achieve this aim, we have re-engineered the R402A enzyme so that access of water to position B is sterically prohibited, with the intention of forcing a water molecule into position A. In this paper, we report the construction and kinetic and crystallographic characterization of the Q363F single-mutant and Q363F/R402A double-mutant flavocytochromes c_3. The structure of the Q363F/R402A enzyme reveals the existence of a water molecule at the active site of the enzyme which is indeed capable of assuming the role of an active site acid catalyst, while the structure of the Q363F single-mutant enzyme reveals the origin of its unexpected kinetic characteristics.

MATERIALS AND METHODS

DNA Manipulation, Strains, Media, and Growth. The mutant enzymes Q363F and Q363F/R402A Fcc_3 were generated using the QuikChange XL Site-Directed Mutagenesis Kit (Stratagene). In the case of the Q363F mutation, the template for the reaction was pEGX1 (WT *fccA*/pMMB503EH) (*3*), while for the Q363F/R402A mutation, the template was pCM68 (R402A *fccA*/pMMB503EH) (*9*).

Oligonucleotides were designed to incorporate the glutamine 363 to phenylalanine change and were complementary to the same sequence on both strands of the plasmid: GAAAGACATGCAGTATATCTTCGCTCACCCAACACTATCTG (complementary to the antisense strand) and CAGATAGTGTTGGGTGAGCGAAGATATACTGCATGTCTTTC (complementary to the sense strand). Mismatched bases are underlined. Temperature cycling, product digestion with *Dpn*I, and transformation of *E. coli* XL-10 Gold ultracompetent cells were carried out as per the Stratagene protocol. Plasmid DNA (Q363F *fccA*/pMMB503EH, pCM138; Q363F+R402A *fccA*/pMMB503EH, pCM139) was screened for the required mutation using an ABI Prism 3100 genetic analyzer, and the mutated *fccA* coding sequence was similarly sequenced to verify that no secondary mutations had been introduced. Expression in Δ*fccA S. frigidimarina* strain EG301 (*3*) was carried out as described previously (*9*).

Protein Purification and Kinetic Analysis. Wild-type and mutant forms of flavocytochrome c_3 were purified as previously reported (*11*). Protein samples for crystallization and mass spectrometry were subjected to an additional purification step using FPLC with a 1 mL Resource Q column (Pharmacia) as described by Pealing et al. (*12*). Protein concentrations were determined using the Soret band absorption coefficient for the reduced enzyme (752.8 mM^{-1} cm^{-1} at 419 nm) (*11*).

The FAD content of Fcc_3 mutants was determined using the method of Macheroux (*13*), and all steady-state rate constants were corrected for the percentage of FAD present.

Mass spectrometry of proteins was carried out using a Micromass Platform II Electrospray mass spectrometer. Samples were prepared in 0.1% formic acid and introduced into the spectrometer via direct infusion. The spectrometer was standardized using horse heart myoglobin.

The steady-state kinetics of fumarate reduction were followed at 25 °C as described by Turner et al. (*14*). The fumarate-dependent reoxidation of reduced methyl viologen was monitored at 600 nm using a Shimadzu UV-PC 1501 spectrophotometer. To ensure anaerobicity, the spectrophotometer was housed in a Belle Technology glovebox under a nitrogen atmosphere with the O_2 level maintained well below 2 ppm. Assay buffers contained 0.45 M NaCl and 0.2 mM methyl viologen and were adjusted to the appropriate pH values using 0.05 M HCl or NaOH as follows: Tris-HCl (pH 7.0−9.0), MES/NaOH (pH 5.4−6.8), and CHES/NaOH (pH 8.6−10). The viologen was reduced by addition of sodium dithionite until a reading of ∼1 absorbance unit was obtained (corresponding to ∼80 μM reduced methyl viologen). The concentration of reduced methyl viologen could be varied between 100 and 20 μM with no effect on the rate of reaction. A known concentration of enzyme was added and the reaction initiated by addition of fumarate.

Kinetic parameters K_M and k_{cat} were determined from the steady-state results using nonlinear regression analysis (Microcal Origin software).

Crystallization and Refinement. Crystallization of Q363F and Q363F/R402A flavocytochrome c_3 was carried out by hanging drop vapor diffusion at 4 °C in Linbro plates. Crystals were obtained with well solutions comprising 100 mM Tris-HCl buffer (pH 7.8−8.5) (measured at 25 °C), 80 mM NaCl, 16−19% PEG 8000, and 10 mM fumarate. Hanging drops 4 μL in volume were prepared by adding 2 μL of 6 mg/mL protein [in 10 mM Tris-HCl (pH 8.5)] to 2 μL of well solution. After approximately 10 days, needles of up to 1 mm × 0.2 mm × 0.2 mm and plates of up to 0.5 mm × 0.5 mm × 0.2 mm were formed. Crystals were immersed in a solution of 100 mM sodium acetate buffer

Table 1: Kinetic Parameters for Fumarate Reduction in Wild-Type, Q363F, and Q363F/R402A Flavocytochromes c_3

	k_{cat} (s^{-1})			K_M (μM)		
pH	wild type[a]	Q363F/R402A	Q363F	wild type[a]	Q363F/R402A	Q363F
6.0	658 ± 34	0.064 ± 0.001	0.26 ± 0.01	43 ± 10	6.6 ± 0.6	843 ± 102
7.2	509 ± 15	0.332 ± 0.007	1.34 ± 0.05	25 ± 2	5.0 ± 0.6	999 ± 132
7.5	370 ± 10	0.420 ± 0.012	1.64 ± 0.05	28 ± 3	5.3 ± 0.8	1064 ± 115
9.0	210 ± 13	0.278 ± 0.007	1.61 ± 0.06	7 ± 2	3.3 ± 0.5	1407 ± 160

[a] Values for the wild-type enzyme taken from ref *9*.

(pH 6.5), 20% PEG 8000, 10 mM fumarate, and 80 mM NaCl, containing 23% glycerol as a cryoprotectant, prior to mounting in nylon loops and flash-cooling in liquid nitrogen. For the Q363F mutant enzyme, crystal data were collected to 1.8 Å resolution at SRS Daresbury (station 9.6, $\lambda = 0.87$ Å) using an ADSC Quantum 4 ccd detector, and for Q363F/R402A, crystal data were collected to 2.0 Å resolution at DESY in Hamburg, Germany (station BW7B, $\lambda = 0.8459$ Å), using a Mar Research mar345 image plate detector. Crystals of both enzymes were found to belong to space group $P2_1$. The Q363F single mutant was found to have the following cell dimensions: $a = 78.520$ Å, $b = 88.886$ Å, $c = 91.194$ Å, and $\beta = 104.42°$; the Q363F/R402A double mutant was found to have the following cell dimensions: $a = 77.971$ Å, $b = 88.280$ Å, $c = 90.087$ Å, and $\beta = 103.89°$.

Data processing was carried out using the HKL package (*15*). The wild-type Fcc_3 structure (1QJD), stripped of water, was used as the initial model for molecular replacement. Electron density fitting was carried out using the program TURBO-FRODO (*16*). Restraints for the FAD were calculated from two small molecule crystal structures (Cambridge Crystallographic Database codes HAMADPH and VEFHUJ10). Structure refinement was carried out using Refmac (*17*).

The atomic coordinates have been deposited in the Protein Data Bank [entries 1LJ1 (Q363F/R402A) and 1M64 (Q363F)].

RESULTS

Characterization of the Mutant Enzyme. The molecular masses of the Q363F and Q363F/R402A mutant enzymes were determined by electrospray mass spectrometry. In comparison to the wild type (63 033 Da), the mass difference was found to be −65 Da for the Q363F/R402A enzyme (expected difference of −66 Da) and 19 Da for the Q363F enzyme (expected difference of 19 Da). Both mutations were further verified by DNA sequencing. The average FAD contents of the Q363F and Q363F/R402A mutant enzymes were found to be 73 and 80%, respectively. This is equivalent to the typical values for the recombinant wild-type enzyme of ~73%. All catalytic rates were corrected for the variation in FAD content.

The ability of the two mutant flavocytochromes c_3 to catalyze fumarate reduction was determined over a range of pH values. The resulting k_{cat} and K_M parameters for the wild-type and mutant forms of Fcc_3 are compared in Table 1. Unlike the R402A single mutant, the Q363F/R402A enzyme does exhibit measurable fumarate reductase activity, albeit with a k_{cat} some 10^3-10^4-fold lower (depending on pH) than that seen for the wild-type enzyme. In terms of K_M, values for the Q363F/R402A enzyme are ~5-fold lower than those of the wild type, decreasing slightly with increasing pH. In the case of the Q363F single-mutant enzyme, values of k_{cat} are ~10^3-fold lower than in the wild-type enzyme, but with hugely elevated K_M values in the millimolar region that would indicate significant impairment of Michaelis complex formation.

Table 2: Data Collection and Refinement Statistics

	Q363F/R402A	Q363F
resolution (Å)	15.0−2.0	15.0−1.8
total no. of reflections	412535	604721
no. of unique reflections	75611	108491
completeness (%)	94.5	96.6
$I/[\sigma(I)]$	9.2	15.8
R_{merge} (%)[a]	7.2	6.2
R_{merge} in outer shell (%)	22.6 (2.07−2.00)	17.6 (1.86−1.80)
R_{cryst} (%)[b]	16.08	16.30
R_{free} (%)[b]	23.47	22.37
rmsd from ideal values		
bond lengths (Å)	0.013	0.012
bond angles (deg)	2.7	2.3
Ramachandran analysis		
most favored (%)	88.6	88.4
additionally allowed (%)	11.3	11.4

[a] $R_{merge} = \sum_h\sum_i|I(h) - I_I(h)|/\sum_h\sum_i I_I(h)$, where $I_I(h)$ and $I(h)$ are the ith and mean measurements of reflection h, respectively. [b] $R_{cryst} = \sum_h|F_o - F_c|/\sum_h F_o$, where F_o and F_c are the observed and calculated structure factor amplitudes of reflection h, respectively. R_{free} is the test reflection data set, 5% selected randomly for cross validation during crystallographic refinement.

Crystal Structure of Q363F and Q363F/R402A Mutant Flavocytochrome c_3. For the Q363F and Q363F/R402A mutant enzymes, data sets to resolutions of 1.8 and 2.0 Å, respectively, were used to refine the structures to final R-factors of 16.30% ($R_{free} = 22.37\%$ for Q363F) and 16.08% ($R_{free} = 23.47\%$ for Q363F/R402A) (see Table 2). For each mutant enzyme, there are two independent molecules in the asymmetric unit and the final model consists of two protein molecules, each comprised of residues 1−568, four hemes, the FAD, one substrate molecule (fumarate), and one sodium ion. In addition, the Q363F model contains 2111 water molecules and the Q363F/R402A model 1630 water molecules. For each protein molecule, three residues at the C-terminus (569−571) could not be located in the electron density maps. The rmsd fit of all backbone atoms for the wild-type and Q363F/R402A mutant flavocytochromes c_3 is 0.3 Å, indicating no major differences between the structures, while the rmsd fit for all backbone atoms for the wild-type and Q363F mutant enzymes is 0.6 Å, indicating greater differences as a result of the single Q363F substitution. Due to the fact that there are two molecules in the asymmetric unit for each structure, the stated rmsd fit value is the average over both molecules (A and B). The rmsd fit of all backbone atoms between molecules A and B within each model is 0.2 Å.

On comparison of the crystal structure of the Q363F/R402A mutant enzyme (Figure 2) with those of the wild-

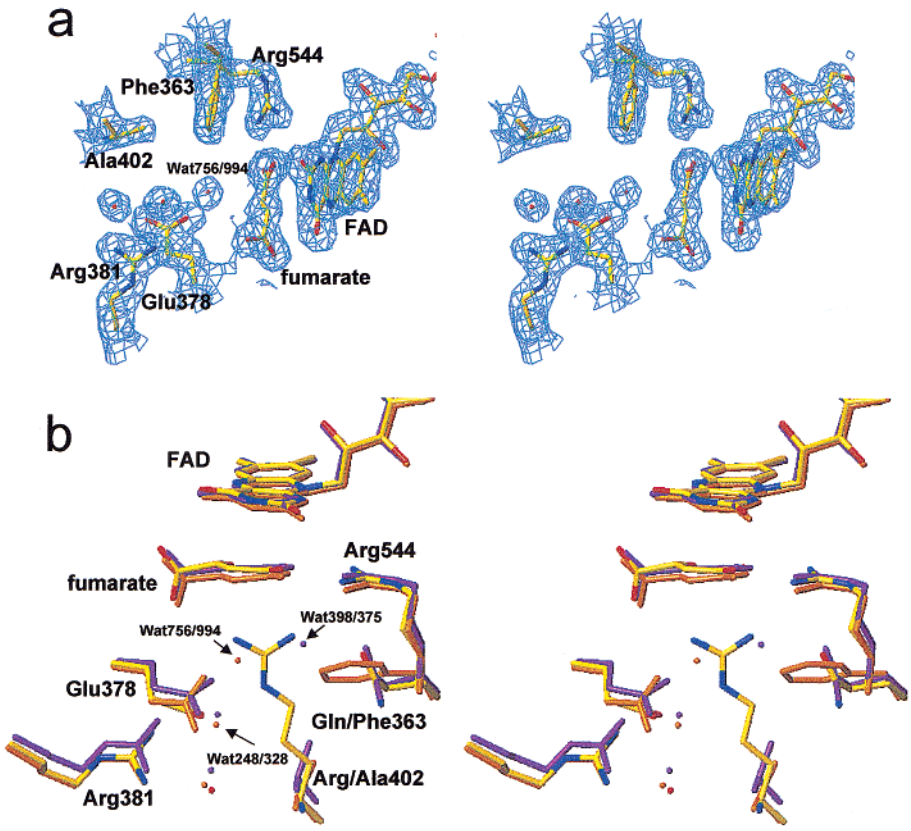

FIGURE 2: Panel a shows a stereodiagram of the active site of the Q363F/R402A double-mutant flavocytochrome c_3. The water which acts as the active site acid catalyst can be clearly seen adjacent to the bound substrate. Electron density was computed using the Fourier coefficients $2F_o - F_c$, where F_o and F_c are the observed and calculated structure factors, respectively, the latter based on the final model. The contour level is 1σ, where σ is the rms electron density. Panel b shows an overlay of the active sites of the wild-type (atom color), R402A (purple), and Q363F/R402A (orange) flavocytochromes c_3. The catalytic water in the Q363F/R402A mutant enzyme can be seen occupying the space designated as position A, which is occupied by one of the NH2 groups of Arg402 in the wild-type enzyme, while the water in the R402A mutant enzyme active site occupies the space taken by the other Arg402 NH2 group in the wild-type enzyme known as position B. The proton pathway residues (Arg381 and Glu378) are also shown, along with the water molecules in the two mutant enzyme structures which result from the movement of the Glu378 side chain in each. This diagram was generated using TURBO-FRODO (*16*).

type enzyme and the R402A single-mutant enzyme, it is clear that there are no unexpected structural changes as a result of the mutation. The phenyl ring of Phe363 is found to occupy the space around position B vacated by the substitution of Arg402 with alanine. What is also apparent is the introduction of a water molecule adjacent to the bound fumarate in both protein molecules of the asymmetric unit (WAT756 in molecule A and WAT994 in molecule B) some 3.5 Å from C3 of the substrate. This water molecule is 3.0 Å from another water molecule (WAT248 in molecule A and WAT328 in molecule B) and 2.7 Å from the carboxylate group of the side chain of Glu378. Glu378 is one of the residues of the proposed proton delivery pathway (Figure 2b). The water molecule which is found at position B in the active site of the R402A single-mutant enzyme (WAT398 in molecule A and WAT375 in molecule B), which forms hydrogen bonding interactions with the side chain of Gln363 and the fumarate C4 carboxylate group, is absent in the structure of the Q363F/R402A double mutant. This absence is due to the steric bulk of the phenylalanine side chain (Figure 2b). The substrate, fumarate, is bound in the same twisted conformation observed in the structure of the wild-type enzyme and other mutant forms of flavocytochrome c_3 (*6*, *9*, *10*). Also, the hydride transfer distance from C2 of fumarate to N5 of the FAD isoalloxazine ring is 3.4 Å, the same as observed in the wild-type and R402A enzyme structures. The integrity of the proton transfer pathway involving residues Arg381 and Glu378 is slightly compromised by the rotation and movement of Glu378 in occupying some of the space vacated by the removal of Arg402, and this movement, similar to that observed in the structure of the R402A mutant flavocytochrome c_3, results in a distance of 4.5 Å between the side chains of Arg381 and Glu378 (compared to 3.1 Å in the wild-type enzyme). However, as a consequence of this change in the orientation of Glu378, a water molecule (WAT248 in molecule A and WAT328 in molecule B) is introduced between Glu378 and Arg381 2.9 Å from Arg381 and 3.8 Å from Glu378, which may serve to mediate in the proton delivery mechanism.

Comparison of the crystal structure of the Q363F mutant enzyme with that of the wild-type enzyme reveals some important changes at the active site as a result of the substitution (Figure 3). The phenyl ring at position 363 can clearly be seen, but it is apparent that the introduction of this steric bulk at the active site has caused Arg402 to swing away from the active site toward the surface of the protein where the guanidinium group resides between Gln201 and Lys404; this has led to significant changes in backbone position between residues Ile399 and Ala405. These changes have allowed a water molecule (WAT300 in molecule A and WAT399 in molecule B) to enter the active site and bind adjacent to the substrate, in position A, 3.4 Å from the

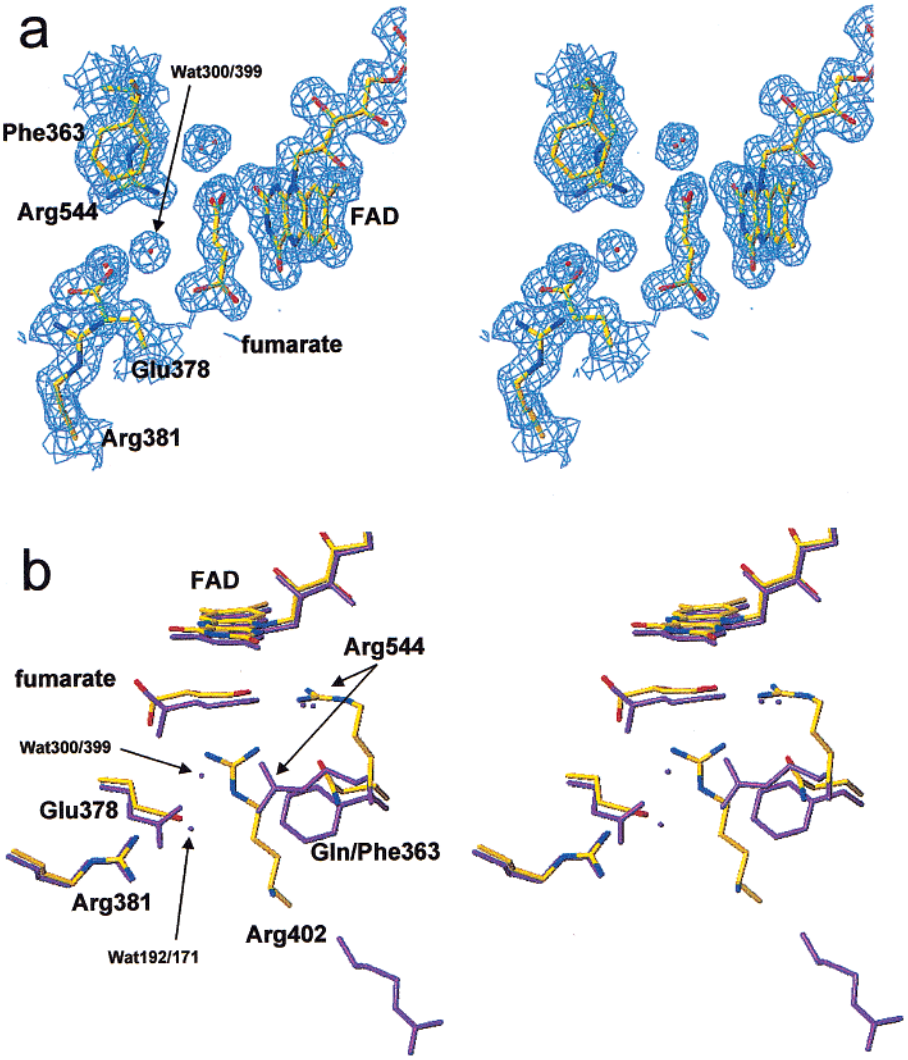

FIGURE 3: Panel a shows a stereodiagram of the active site of the Q363F mutant flavocytochrome c_3. The water which acts as the active site acid catalyst can be clearly seen adjacent to the bound substrate. Electron density was computed using the Fourier coefficients $2F_o - F_c$, where F_o and F_c are the observed and calculated structure factors, respectively, the latter based on the final model. The contour level is 1σ, where σ is the rms electron density. Panel b shows an overlay of the active sites of the wild-type (atom color) and Q363F (purple) flavocytochromes c_3. The side chain of Arg402 in the Q363F mutant enzyme is seen at the bottom right of the figure, and the catalytic water in the Q363F mutant enzyme can be seen occupying the space designated as position A. The movement of Arg544 is also obvious, and the two resulting water molecules are shown adjacent to the fumarate C4 carboxylate group. This diagram was generated using TURBO-FRODO (*16*).

fumarate C3 atom. As in the Q363F/R402A structure, this water is found to be close to the side chain of Glu378 (2.7 Å), and the slight movement of Glu378 has allowed another water molecule (WAT192 in molecule A and WAT171 in molecule B) to bind 3.6 Å from the Glu378 side chain and 2.9 Å from the Arg381 side chain (as seen in the double-mutant enzyme structure); this may mediate the proton delivery process.

In addition to these changes, Arg544, a residue that is important for the formation of the Michaelis complex, has moved to occupy some of the space vacated by the reorientation of Arg402, exhibiting a stacking interaction with Phe363 and a hydrogen bonding interaction with the water molecule located at position A (2.9 Å). The Arg544 side chain is also found to be 3.2 Å from the C4 carboxylate moiety of the bound fumarate. This movement of Arg544 has resulted in the introduction of a further two water molecules, each forming a hydrogen bonding interaction with one of the fumarate C4 carboxylate oxygen atoms.

DISCUSSION

The mechanism for the Fcc_3-catalyzed reaction, as originally proposed by Taylor et al. (*6*), is shown in Figure 4a, and we believe that this mechanism operates throughout the family of fumarate reductase enzymes. The role of Arg402 as the active site acid catalyst has been confirmed by mutagenesis experiments, and its efficiency in this role is explained in terms of its unique ability to simultaneously occupy positions A and B at the active site of the enzyme and act as both a Brønsted acid and a Lewis acid at each site (*10*). This is corroborated by recent work on a related enzyme, L-aspartate oxidase from *E. coli*, which is structurally similar to fumarate reductase and in which Arg290, the residue equivalent to Arg402 in flavocytochrome c_3, acts as the active site base, abstracting a proton from the substrate during catalysis (*18*).

Substitution of Arg402 with alanine in flavocytochrome c_3 leads to an enzyme which has no measurable catalytic activity. This is attributed to the lack of a species capable of

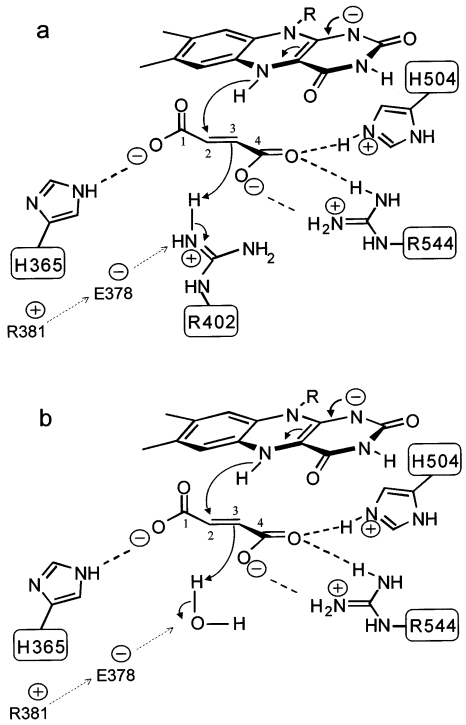

FIGURE 4: Panel a shows the reaction mechanism for fumarate reduction in the wild-type enzyme [this is an abbreviated version of the mechanism proposed by Taylor et al. (*6*)]. The substrate is polarized by interactions with charged residues facilitating hydride transfer from N5 of the reduced FAD to C2 of the substrate. Arg402 is ideally positioned to donate a proton to C3 of the substrate, resulting in the formation of succinate. Arg402 is immediately reprotonated via a proton pathway involving Arg381 and Glu378. Panel b shows the mechanism of fumarate reduction in the Q363F/R402A double-mutant enzyme. The water molecule introduced at position A of the mutant enzyme is shown to function as the active site acid catalyst as part of the proton delivery pathway.

proton transfer in position A of the active site. In this case, however, a water molecule is found in position B, hydrogen bonding with the side chain of Gln363 and the C4 carboxylate group of the bound fumarate. Clearly, it is these hydrogen bonding interactions which result in the preferential occupation of position B in the R402A mutant enzyme, with steric constraints precluding the simultaneous occupation of position A by a second solvent molecule. The construction of the double-mutant enzyme incorporating the R402A substitution in conjunction with the introduction of phenylalanine at position 363 was designed to force a water molecule to preferentially occupy position A rather than position B (Figure 5). Since water is capable of acting as a Brønsted acid, its occupancy of position A should permit fumarate reductase activity to occur via the mechanism shown in Figure 4b. The kinetic and structural characterization of the Q363F/R402A flavocytochrome c_3 confirmed both the presence of the water molecule at position A and its ability to function as an acid catalyst, albeit with a low level of activity. The fact that the k_{cat} value for the Q363F/R402A enzyme is some 1000-fold lower than that seen for the wild-type enzyme could, at least in part, be due to the inability of water to function as a Lewis acid. There may also be an effect arising from the observed perturbation in the relative positions of "proton pathway" residues Arg381 and Glu378.

Construction of the Q363F single-mutant enzyme as a control has proven to be illuminating, leading to a mutant

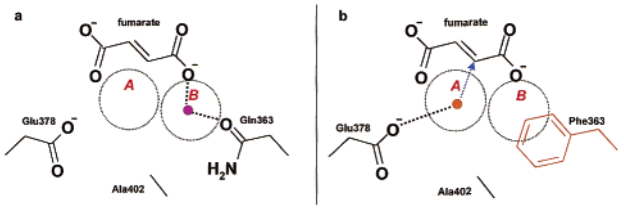

FIGURE 5: Schematic representation of positions A and B in the active site of (a) R402A and (b) Q363F/R402A mutant flavocytochrome c_3. The water in position B of the R402A mutant enzyme is shown in purple, while the water in position A of the Q363F/R402A enzyme is shown in orange along with Phe363. Hydrogen bonding interactions are shown as dashed lines. The direction of proton transfer in Q363F/R402A flavocytochrome c_3 is shown using a blue arrow.

enzyme with unexpected characteristics. Although the enzyme was found to display fumarate reductase activity at a low level, the high K_M value for fumarate results in an inefficient enzyme (in terms of k_{cat}/K_M). In this case, the crystal structure that was obtained has been crucial in accounting for the kinetic observations, showing that Arg402, the active site acid, has moved away from the active site as a result of the introduction of a phenylalanine residue at position 363. This has allowed a water molecule to occupy position A of the active site in the mutant enzyme, resulting in the measured fumarate reductase activity. In addition, Arg544, a residue that is important for substrate binding, has moved into the active site, and is no longer involved in the Michaelis complex formation, thus explaining the high substrate K_M value that is observed. Interestingly, the value of k_{cat} measured for the Q363F mutant enzyme is ~3-fold greater than that seen with the Q363F/R402A double-mutant form.

In conclusion, by generating the Q363F/R402A double-mutant form of flavocytochrome c_3, we have succeeded in the novel engineering of a water molecule as the active site acid in a fumarate reductase.

REFERENCES

1. Iverson, T. M., Luna-Chavez, C., Cecchini, G., and Rees, D. C. (1999) *Science 284*, 1961−1966.
2. Körtner, C., Lauterbach, F., Tripier, D., Unden, G., and Kröger, A. (1990) *Mol. Microbiol. 4*, 855−860.
3. Gordon, E. H. J., Pealing, S. L., Chapman, S. K., Ward, F. B., and Reid, G. A. (1998) *Microbiology 4*, 937−945.
4. Lancaster, C. R. D., Kröger, A., Auer, M., and Michel, H. (1999) *Nature 402*, 377−385.
5. Lancaster, C. R. D., Gross, R., and Simon, J. (2001) *Eur. J. Biochem. 268*, 1820−1827.
6. Taylor, P., Pealing, S. L., Reid, G. A., Chapman, S. K., and Walkinshaw, M. D. (1999) *Nat. Struct. Biol. 6*, 1108−1112.
7. Leys, D., Tsapin, A. S., Nealson, K. H., Meyer, T. E., Cusanovich, M. A., and Van Beeumen, J. J. (1999) *Nat. Struct. Biol. 6*, 1113−1117.
8. Bamford, V., Dobbin, P. S., Richardson, D. J., and Hemmings, A. M. (1999) *Nat. Struct. Biol. 6*, 1104−1107.
9. Doherty, M. K., Pealing, S. L., Miles, C. S., Moysey, R., Taylor, P., Walkinshaw, M. D., Reid, G. A., and Chapman, S. K. (2000) *Biochemistry 39*, 10695−10701.
10. Mowat, C. G., Moysey, R., Miles, C. S., Leys, D., Doherty, M. K., Taylor, P., Walkinshaw, M. D., Reid, G. A., and Chapman, S. K. (2001) *Biochemistry 40*, 12292−12298.
11. Pealing, S. L., Cheesman, M. R., Reid, G. A., Thomson, A. J., Ward, F. B., and Chapman, S. K. (1995) *Biochemistry 34*, 6153−6158.

12. Pealing, S. L., Lysek, D. A., Taylor, P., Alexeev, D., Reid, G. A., Chapman, S. K., and Walkinshaw, M. D. (1999*) J. Struct. Biol. 127*, 76−78.
13. Macheroux, P. (1999) in *Flavoprotein Protocols: Methods in Molecular Biology* (Chapman, S. K., and Reid, G. A., Eds.) Vol. 131, pp 1−7, Humana Press, Totowa, NJ.
14. Turner, K. L., Doherty, M. K., Heering, H. A., Armstrong, F. A., Reid, G. A., and Chapman, S. K. (1999) *Biochemistry 38*, 3302−3309.
15. Otwinowski, Z., and Minor, W. (1997) *Methods Enzymol. 276*, 307−326.
16. Roussel, A., and Cambillau, C. (1991) TURBO-FRODO, in *Silicon Graphics Geometry Partners Directory 86*, Silicon Graphics, Mountain View, CA.
17. Murshudov, G. N., Vagin, A. A., and Dodson, E. J. (1997) *Acta Crystallogr. D53*, 240−255.
18. Bossi, R. T., Negri, A., Tedeschi, G., and Mattevi, A. (2002) *Biochemistry 41*, 3018−3024.

BI0203177